Discontinuities in the Center Conductor of Symmetric Strip Transmission Line*

H. M. ALTSCHULER† AND A. A. OLINER†

Summary—A systematic measurements program has been carried out to check the validity of theoretical formulas for the equivalent circuit parameters of a variety of discontinuities in the center conductor of symmetric strip transmission line. These theoretical formulas have been in part previously available and are in part new or modified. Results indicate that, in general, these formulas are adequate for most engineering purposes and that certain of the network parameters can be neglected.

I. Introduction

THEORETICAL expressions for the equivalent circuit parameters of a variety of discontinuity structures in the center conductor of strip transmission line have been available[1] for some time now. Many of these are simple, first order results derived from known formulas for the equivalent circuit parameters of related microwave structures. While some of these theoretical expressions had been compared with measurements in the past,[2,3] many had not been checked. The work described here, which was initiated some years ago, has been a systematic effort to fill this gap. It has thrown light on the accuracy of the formulas in question and, in addition, has resulted in the modification of certain of these formulas (Section III-I) and in the derivation of expressions not available heretofore (Sections III-B, D, and G).

The emphasis is placed on the comparison between theory and measurement. The many techniques and details involved in carrying out the construction of the center strips, in the measurement techniques, and in the network considerations required to cast the measured data into usable form are largely omitted. These points have been adequately discussed in a thesis.[4]

A brief description of the apparatus used, the nature of the center strip, and some comments on the precision employed follow immediately below. The balance of the report, after brief general remarks, is devoted to the comparison of theory with measurements for a variety of discontinuity structures. Each type of discontinuity is treated in a separate self-contained section which includes the theoretical formulas used, an indication of their derivation, comments on the representation employed, graphs comparing theory and measurement, and a discussion of the results obtained.

II. The Measurement Apparatus

In outline, the measurement equipment is a standard impedance measuring setup consisting of a source, a standing wave indicator followed by the discontinuity, which in turn is terminated in a variable short circuit. All components but the source were incorporated into a single unit [shown in Fig. 1(a) and (b)] which is

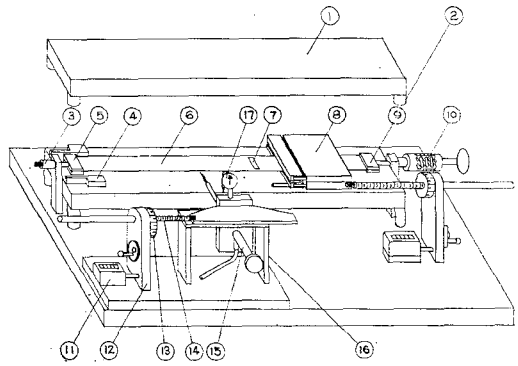

1	UPPER GROUND PLATE	5	INPUT CLAMP	9	END CLAMP	13	VERNIER	17	DIAL GAUGE
2	SUPPORT	6	STRIP	10	TENSION SPRING	14	DRIVING SCREW		
3	INPUT CONNECTOR	7	DISCONTINUITY	11	REVOLUTION COUNTER	15	PROBE		
4	MODE SUPPRESSOR	8	CHOKE SHORT CIRCUIT	12	GEAR TRAIN	16	STANDING WAVE METER		

(a)

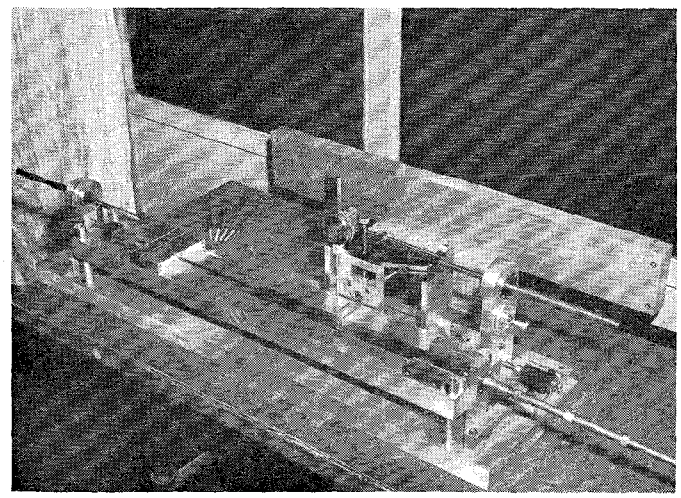

(b)

Fig. 1—Measurement apparatus. (a) Sketch of front view. (b) Photograph of back view.

* Manuscript received by the PGMTT, November 24, 1959; revised manuscript received, January 18, 1960. The research reported was conducted under Contract No. AF-19(604)-2031 sponsored by the Air Force Cambridge Res. Center, Air Res. and Dev. Command.

† Microwave Res. Inst., Polytechnic Institute of Brooklyn, Brooklyn 1, N. Y.

[1] A. A. Oliner, "Equivalent circuits for discontinuities in balanced strip transmission line," IRE Trans. on Microwave Theory and Techniques, vol. MTT-3, pp. 134–143; March, 1955.

[2] A. D. Frost, private communication, Tufts University, Medford, Mass.; April 30, 1954.

[3] H. S. Keen, "Scientific Report on Study of Strip Transmission Lines," Airborne Instruments Lab., Mineola, N. Y., Rept. No. 2830-2; December, 1955.

[4] M. S. Stillman, "Measurement of Discontinuities in Symmetric Strip Transmission Line," M.E.E. thesis, Polytechnic Institute of Brooklyn, N. Y.; June, 1958.

described here to indicate the care with which the measurements were carried out.

The equipment is unique in that its center conductor is a flat, thin strip which is suspended in tension between an input connector and a spring-loaded clamp at the other end of the ground plates. This feature was chosen so that the center strip can be completely surrounded by air. These conditions correspond closely to the assumptions underlying the theoretical formulas that the center strip is of zero thickness and is immersed in a single homogeneous medium. An operating frequency of 1500 mc and a characteristic impedance of 50 ohms with a center conductor width of 1.5 inches and a plate spacing of 1.051 inches were chosen. Such large dimensions were employed to reduce mechanical problems and to increase accuracy.

The equipment is shown from two different views in Fig. 1(a) and (b). The upper ground plate is shown in an exploded view. All the equipment is mounted on a sturdy base plate. The two carefully machined aluminum ground plates are supported by cylindrical spacers. The center conductor of the input connector ends in an input clamp which has been made as small as possible to keep the associated discontinuity reasonably low. An interchangeable center strip, which includes the discontinuity, runs from the input clamp to the end clamp. The two mode suppressor plates near the input discriminate strongly against the radiating (parallel plate) TEM mode in that the dominant rectangular guide mode in this region is well beyond cutoff. The standing-wave meter incorporates a side probing arrangement similar to that used by Cohn.[5] It is driven by a gear train with an associated revolution counter and a wheel vernier with a ± 0.0001-inch readability. A conventional probe, modified by extending the probe wire and its shield by several inches, was used. The probe can also be moved in a vertical direction with respect to the probe carriage, and its distance from the bottom ground plate can be measured by means of a dial gauge. The standing-wave meter and the associated equipment are mounted on a small separate base plate which can be rotated slightly by means of adjustment screws in order to bring the probe travel into parallelism with the center strip. The movable choke-type short circuit has associated with it the same type of drive and counter mechanism as the standing-wave meter. It is built in the form of a "sandwich" about the center strip and is guided by a groove in the bottom ground plate. The top "half" of the short circuit is removable to allow the center conductor to be changed. The end clamp holds the center strip and transmits the force of the (variable) tension spring to the center strip.

Center strip construction was originally the subject of much experimentation with the object of reducing or eliminating undesirable deformations which occur in the neighborhood of the discontinuity when the strips are in tension. The construction finally arrived at includes a 0.001-inch "Mylar" polyester film (no discontinuity is cut in this) sandwiched between two 0.001-inch copper foil strips. After assembly with a tacky teflon cement, the total thickness is about 0.0035 inch. In order to minimize deformation, tension in the copper is relieved by certain cuts made near the discontinuity (perpendicular to the direction of force) across the copper strips. Before measurements were made, the strips were stress relieved in tension for a number of hours. Both "cutting" and photo-etching techniques were employed in constructing discontinuities.

The over-all performance of the measurement setup was satisfactory. Excessive radiation was guarded against by careful strip construction techniques and by centering the strip between the plates with utmost care. Inevitably, there remained a very small amount of radiation which did not appear to influence the measurements at all. The quality of the measurements is reflected by such typical insertion VSWR values as $|\gamma| = 1.167 \pm 0.006$, $|\gamma| = 1.422 \pm 0.008$ and $|\gamma| = 148 \pm 1.5$. The curve of Fig. 2 shows the plotted data ($D+S$ vs S) for a typical step discontinuity together with a plot of the scatter (ΔD vs S) which remained after the network parameters were abstracted by analytical means. To emphasize how small the scatter is in relation to the data, $D+S$ and ΔD are shown to the same scale. In the region of $|\gamma|$ near 1.5 the uncertainties ranged from 0.006 to 0.010; in the same region of $|\gamma|$ the uncertainties associated with precision X-band equipment used to measure discontinuities in rectangular waveguide ranged from 0.002 to 0.007. This is viewed as an indication of very good precision when the construction and mounting difficulties are kept in mind. The errors associated with the necessary reference plane measurements were unfortunately considerably larger. These are thought to have been of the order of ± 0.020 inch, *i.e.*, about $\pm \lambda/400$. These errors, though not serious, made themselves quite evident in parameters which were sensitively dependent on reference plane location.

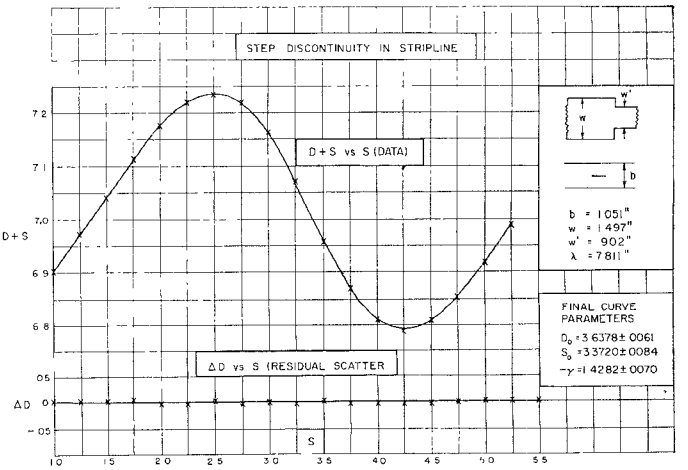

Fig. 2—Typical data curve and associated residual scatter.

[5] S. B. Cohn, "Problems in strip transmission line," IRE Trans. on Microwave Theory and Techniques, vol. MTT-3, pp. 119–126; March, 1955.

III. Comparison Between Theory and Measurement

A. General Remarks

The measurements described in the following were all carried out at very nearly 1500 mc, *i.e.*, at a wavelength of about 7.87 inches, except for the abruptly-ended center conductor (Section III-B) for which measurements were carried out at various frequencies. The cross section of the strip transmission line used is shown in Fig. 3, in which b, w, and t are implicitly defined. The plate spacing b was maintained accurately throughout the measurements, but the strip width w actually varied slightly from strip to strip. These variations were always properly taken into account. Strip thickness t was taken to be zero in all cases but in the calculations of the characteristic impedance ratios of step discontinuities (Section III-F), where this ratio and the measured insertion VSWR were very nearly equal to each other.

The characteristic impedance values used in certain formulas below were obtained from the following known expressions:

$$Z_o = \frac{30\pi\left(1 - \frac{t}{b}\right)}{D/b}\,; \quad Z_{02}/Z_{01} = D_1/D_2 \tag{1}$$

where, for small strip thickness t, D is given accurately by

$$D = bK(k)/K(k') + \frac{t}{\pi}\left[1 - \ln\left(\frac{2t}{b}\right)\right] \tag{2}$$

and, to a very good approximation, for $w/b > 0.5$, by

$$D = w + \frac{2b}{\pi}\ln 2 + \frac{t}{\pi}\left[1 - \ln\left(\frac{2t}{b}\right)\right]. \tag{3}$$

Here k and k' are defined by

$$k = \tanh(\pi w/2b), \qquad k' = (1 - k^2)^{1/2}. \tag{4}$$

In the preceding expressions, D is the "equivalent strip width," *i.e.*, the width of a strip with an associated *uniform* field (without fringing) but with the same capacitance as the actual strip.

Unless stated otherwise, all impedances and reactances are assumed to be properly normalized to characteristic impedance. In other words, the normalized impedance of a matched termination is unity. Normalization is indicated by a prime. All dimensions and lengths are given in inches.

Since the equivalent circuit parameters are expressed in normalized form, these circuits are to be used in the following usual fashion: Impedances which terminate the network must be taken as normalized; any input impedance computed from the network is then automatically normalized. Measured parameters are automatically expressed in normalized terms unless characteristic impedance values are explicitly introduced into the computations which transform the measured data into a network representation.

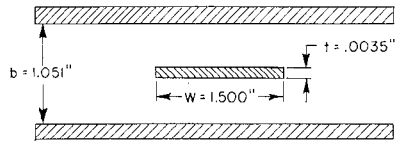

Fig. 3—Cross section of strip transmission line.

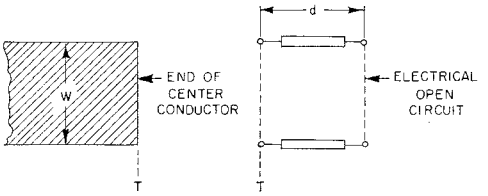

Fig. 4—Abruptly-ended center conductor. (a) Physical structure. (b) Equivalent circuit.

B. Abruptly-Ended Center Conductor

The physical structure and the equivalent network of the abruptly-ended center conductor are shown in Fig. 4. Since, to a crude approximation, one can expect an electrical open circuit to be located at the plane T, the representation chosen results in relatively small values of the transmission line length d for practical strip transmission lines.

The only rigorous theoretical result available for this structure is the known static value for the center conductor of infinite width (fringing at an edge). In this case one has a value of d equal to c where

$$c = \frac{b \ln 2}{\pi}\,. \tag{5}$$

For the case in which the center conductor width w is not infinite, a theoretical expression based on both edge and corner fringing has been developed. The edge contribution is based on the above (infinite width) expression, while the corner contribution has been obtained empirically from measured data since no theoretical solution for the capacitance of a corner between parallel plates is available. The formula is

$$d = \frac{1}{\kappa}\cot^{-1}\left[\frac{4c + 2w}{c + 2w}\cot(\kappa c)\right], \qquad \kappa = \frac{2\pi}{\lambda} \tag{6}$$

where λ is the wavelength in the medium. For most practical dimensions (κc small), one can approximate (6) by (7) which is seen to be independent of κ, *i.e.*, of both the frequency and the dielectric constant of the material contained in the transmission line. The simplified formula is

$$d = c\left(\frac{c + 2w}{4c + 2w}\right), \tag{7}$$

which approximates (6) to within 3 per cent for $\kappa c \leq 0.3$.

Eqs. (6) and (7) already hold implicit the value of the empirically obtained corner fringing capacitance C_{cf}. An independently derived formula for d/b, which explicitly contains the corner fringing capacitance as a parameter, has been available[6] for the case of parallel-coupled strips, one of which is open-ended. In the limit in which the strips become completely uncoupled this expression reduces exactly to the simplified form (7). The symbol C_f'' employed by these authors is defined as one-half of C_{cf}; their empirical value for $2C_f''$ in micromicrofarads for a zero-thickness center strip is $0.019\,\epsilon_r b$, where b is in inches and ϵ_r is the relative dielectric constant. The corresponding value of C_{cf} implicit in (7) is $0.011\,\epsilon_r b$.

Theoretical and experimental values for d, the location of the electrical open circuit with respect to the end of the center conductor, are compared in Fig. 5, in which both strip width (the parameter) and d have been normalized to the plate spacing b. Measurements were made at six different wavelengths ranging from $\lambda = 5.4$ inches to $\lambda = 11.8$ inches. The "bars" crossing the theoretical curves result from both experimental scatter and the small variation of d/b with frequency. The theoretical curve is based on (7). The writers have also been informed[7] that data taken at the Stanford Research Institute and the Airborne Instruments Laboratory over a portion of the ω/b range lie near the upper limit of the vertical scatter lines shown in Fig. 5.

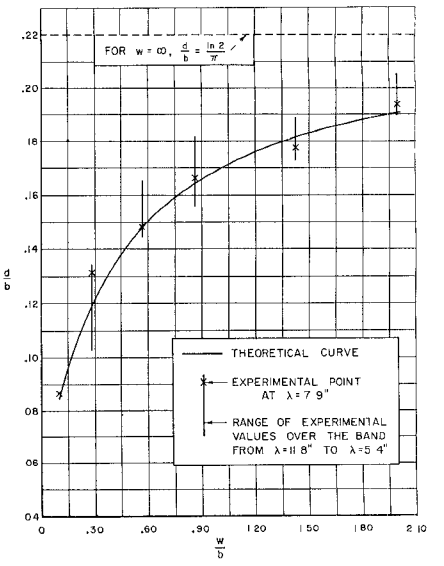

Fig. 5—Location of equivalent open circuit for abruptly-ended center conductor.

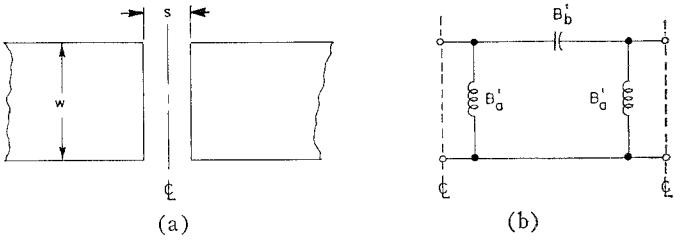

Fig. 6—Gap in center conductor. (a) Physical structure. (b) Equivalent circuit at centerline reference planes.

C. Gap in Center Conductor

The physical gap structure and its equivalent admittance pi network[8] at centerline reference planes are shown in Fig. 6.

The gap formulas[1] were originally derived from available results for E-plane slit-coupled rectangular waveguides. The derivation proceeded by first obtaining an approximate parallel plate waveguide model of the actual discontinuity structure, consisting of two parallel plate waveguides coupled by an infinite slit (gap) of width s, and then by simply employing the known rectangular waveguide result by re-expressing it in the limit as the guide width becomes infinite. As a result of the manner of derivation, the strip width w does not enter as a parameter into the formulas obtained. As w/b becomes very small the formulas can consequently be expected to deteriorate. The expressions are

$$B_a' = -\frac{2b}{\lambda}\ln\left[\cosh\left(\frac{\pi s}{2b}\right)\right], \tag{8}$$

$$B_b' = \frac{b}{\lambda}\ln\left[\coth\left(\frac{\pi s}{2b}\right)\right]. \tag{9}$$

Comparison of theoretical results with measured data furnished by the Airborne Instruments Laboratory was made previously[1] for the case of a 50-ohm line and showed rather good agreement over a wide range of frequencies. Subsequent measurements[9] indicate that for very narrow strips (high characteristic impedances) the values of B_a' and B_b' decrease noticeably. In extreme cases the values predicted by these simple formulas may be too large by a factor of 1.4 for B_a' and 2.0 for B_b'.

D. Rectangular Slot in Center Conductor

The physical slot structure and its equivalent admittance pi network are shown in Fig. 7. The slot is narrow and is centered on the strip conductor; when $d = w$, *i.e.*, when the slot runs completely across the strip, the structure is called a gap. It is known that a narrow gap is capacitive while a short slot is inductive, so that the slot should be resonant for some intermediate length.

[6] S. B. Cohn, *et al.*, "Research on Design Criteria for Microwave Filters," Stanford Res. Inst., Menlo Park, Calif., pp. 115–116; June, 1957.

[7] S. B. Cohn, private communication.

[8] The reviewers point out that many of the inductive network elements, such as those in Figs. 6 and 7, are actually negative capacitive elements and that therefore it is proper to use capacitor rather than inductor symbols in these instances. The authors agree that, to a first order, the formulas for these elements have the frequency dependence of negative capacitance. Nevertheless, the customary symbolism has been retained in this paper for the following reasons: 1) It is not clear whether such network symbols should imply primarily frequency dependence or sign; 2) at any given single frequency the sign is of course more important; 3) if an element is to be used over a frequency band, the detailed expression for the element must be carefully examined in any case, since not all elements possess a simple frequency dependence.

[9] Keen, *op. cit.*, Figs 18 and 19.

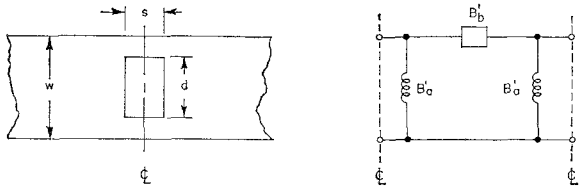

Fig. 7—Slot in center conductor. (a) Physical structure. (b) Equivalent circuit at centerline reference planes.

These remarks apply to the series arm B_b' of the pi equivalent network for the slot. The inductive shunt arms are due to the finite width of the slot, but their effect is small if the slot is narrow.

The hitherto unpublished formulas given below for a slot in the center conductor were derived by Suzuki.[10] Their evaluation is based on the use of the following simple model for the strip transmission line. By replacing the fringing field at the strip edges by an extension of the strip width which is terminated by an open circuit, the strip transmission line is transformed into two parallel plate guides of finite width placed back to back and coupled by the slot. By duality considerations, the geometry is then related to a flat metal rectangle located parallel to the electric field in a parallel plate waveguide of width equal to the *height* of the original strip line. The equivalent circuit for the metal rectangle in parallel plate guide is then obtained approximately from an accurately derived result for a tuned post[7] in rectangular waveguide.

The formulas for the slot are given below. In the limit as the slot runs completely across the center conductor, these complicated formulas reduce exactly to the expressions for the gap given in Section III-C.

$$B_a' = \frac{-\frac{2b}{\lambda}\ln\cosh\frac{w\tau}{b}}{1+P} \tag{10}$$

$$B_b' = -\frac{b}{\lambda}\ln\sinh\frac{w\tau}{b} - \frac{B_a'}{2} - \frac{b\lambda}{w^2}\left(1+\frac{2b}{\pi w}\ln 2\right)Q \tag{11}$$

where

$$Q \simeq \frac{1}{4\tau}\left[\frac{-1}{\ln\beta} - \left(\frac{1-\beta^2}{\ln\beta}\right)^2 \sum_{n=1}^{N} f(2n\tau)\frac{X_n^2}{n}\right].$$

N is the integer nearest the quantity $(0.7/\tau - 1)$,

$$P \simeq \frac{1}{4}\left(\frac{1-\beta^2}{\ln\beta}\right)^2 \sum_{n=1}^{5} g(2n\tau)\frac{X_n^2}{n^2} + \tau^2 Q,$$

and where

$$\tau = \frac{\pi s}{2w} \quad \text{and} \quad \beta = \cos\frac{\pi d}{2w}.$$

The quantity X_n is given by

$$X_1 = 1,\ X_2 = -1 + 3\beta^2,\ X_3 = 1 - 8\beta^2 + 10\beta^4,$$
$$X_4 = -1 + 15\beta^2 - 45\beta^4 + 35\beta^6,$$
$$X_5 = 1 - 24\beta^2 + 126\beta^4 - 224\beta^6 + 126\beta^8.$$

The functions $f(x)$ and $g(x)$ are plotted in Fig. 8. The formulas for B_a' and B_b' are applicable only when $\tau \geq 0.15$ and $d/w \geq 0.25$.

Theoretical and experimental values for the parameters of slots and certain gaps are compared in Fig. 9. It can be seen that these values are in good agreement with each other. The series susceptance B_b' is the dominant parameter in the representation for the slot since the associated values of B_a' are quite small. It is of interest to note that the series susceptance B_b' for the slots considered are all inductive, while B_b' for gaps are capacitive. The curve for $s = 0.155$ shows how rapidly the value of B_b' passes through resonance and that resonance occurs when the slot is "almost a gap." This is well confirmed by the experimental data. It is consequently recognized that a resonant slot is an impractical structure. Quite apart from the high sensitivity of the resonant point to the exact slot dimensions, the slot side walls $(w - d/2)$ would have to be exceptionally thin to obtain resonance and would consequently present virtually insurmountable construction problems.

E. Round Hole in Center Conductor

The physical structure and the equivalent pi network for the round hole in a strip line center conductor are shown in Fig. 10. It should be noted that this representation is at the centerline of this symmetric structure.

The theoretical formulas for B_a' and B_b' have been available for some time[1] and were obtained by means of variational expressions. The stored power terms (numerators) involved were obtained by small aperture considerations from known results for the E-plane aperture coupling of two rectangular waveguides. The formulas are

$$B_b' = -3\lambda b D/4\pi d^3, \tag{12}$$

$$B_a' = 1/4B_b'. \tag{13}$$

Extensive measurements on this discontinuity were carried out at the Airborne Instruments Laboratory, the results of which are already available.[1,3] The theoretical values were found to be in good agreement with the results of the measurements referred to.

F. Step (Change in Width) in Center Conductor

The physical structure and an equivalent network for the step (abrupt change of center conductor width) are shown in Fig. 11. Since both characteristic impedances

[10] M. Suzuki, "Circuit Parameters of a Tuning Post in a Rectangular Waveguide and its Applications," Microwave Res. Inst., Polytechnic Inst. of Brooklyn, N. Y., Rept. No. R-591-57, PIB-519; July, 1957.

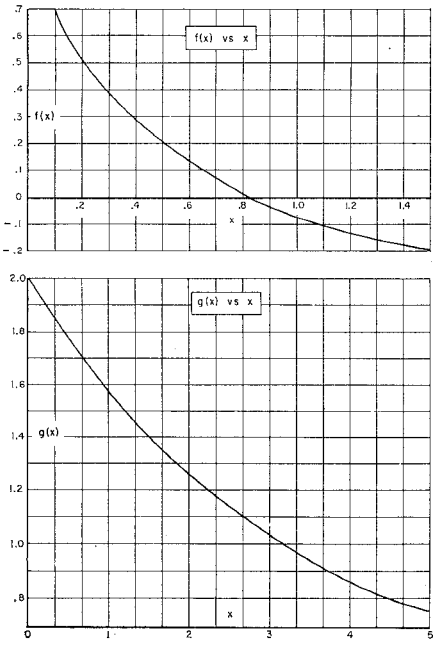

Fig. 8—Functions employed in slot formulas

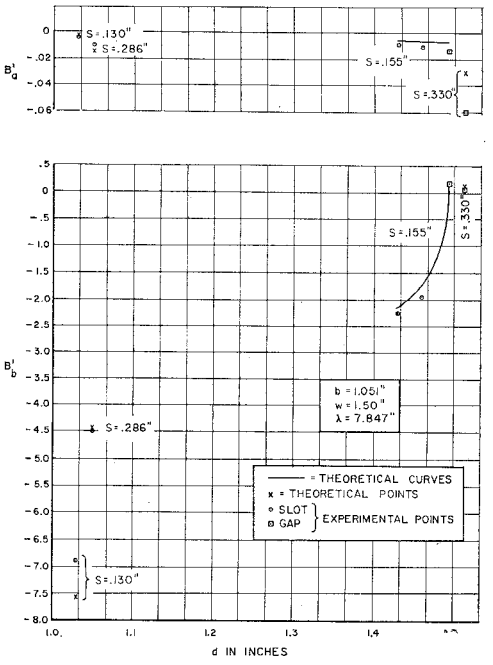

Fig. 9—Circuit parameters of slots and gaps.

have been normalized here by taking them as unity (see Section III-A), the ideal transformer $\sqrt{Z_{02}'}$:1 appears explicitly in the circuit representation. If the (unnormalized) characteristic impedances of the two transmission lines involved are defined as Z_{01} and Z_{02}, respectively, then

$$Z_{02}' = Z_{02}/Z_{01} \quad \text{and} \quad X' = X/Z_{01}.$$

The theoretical formulas (for X', l_1, and l_2) were obtained[1] via a Babinet equivalence procedure from the known parameters of a step in the height of rectangular

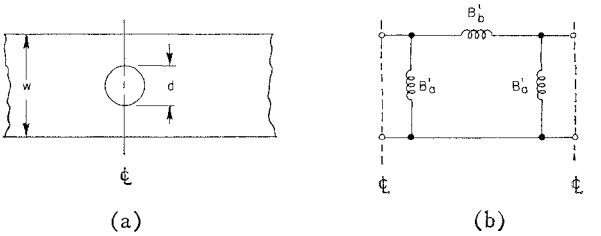

Fig. 10—Round hole in center conductor. (a) Physical structure. (b) Equivalent circuit at centerline reference planes.

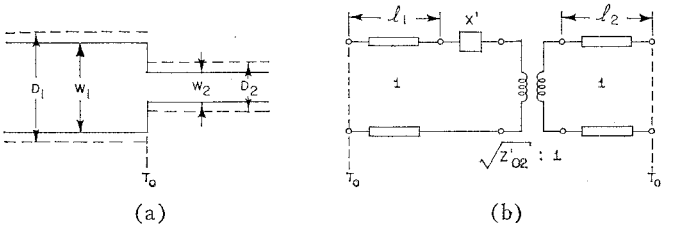

Fig. 11—Step (change in width) in center conductor. (a) Physical structure. (b) Equivalent circuit.

waveguide. The approximation used was such that l_1 and l_2 depend only on the strip-line ground-plate spacing. This simple dependence is certainly open to question, but no more exact formulation has been attempted. The theoretical formulas are

$$X' = \frac{2D_1}{\lambda} \ln \csc\left(\frac{\pi D_2}{2D_1}\right), \tag{14}$$

$$l_1 = -l_2 = \frac{b \ln 2}{\pi}. \tag{15}$$

The values for D_1, D_2, and Z_{02}' are obtained from (1) to (4). The theoretical insertion VSWR for the structure, r, is computed from X' and Z_{02} by the following formula:

$$r = a + \sqrt{a^2 - 1}, \quad \text{where} \quad a \equiv \frac{X'^2 + Z_{02}'^2 + 1}{2Z_{02}'}. \tag{16}$$

Theoretical and experimental values for some of the circuit parameters are presented in Table I. The values

TABLE I

w_2 (inches)	Theoretical			Experimental r	Semi-Experimental (inches)	
	Z_{02}'	r	X'		l_1	l_2
.152	3.375	3.429	.408	3.348 ± .035	+.102	−.102
.310	2.577	2.614	.287	2.614 ± .025	+.063	−.067
.600	1.842	1.857	.142	1.825 ± .013	+.065	−.079
.902	1.436	1.440	.059	1.428 ± .007	+.042	−.065
1.205	1.174	1.175	.014	1.204 ± .018	−.047	+.056

given assume various wavelengths λ very close to 7.80 inches, strip widths w_1 nearly equal to 1.50 inches, and a ground plate spacing maintained at $b > 1.051$ inches. It follows that the theoretical values for the transmission

line lengths l_1 and l_2 are

$$l_1 = -l_2 = 0.232 \text{ inch.}$$

Above all, it will be noted that the theoretical values for Z_{02}' and r, and the experimental values of r, all fall very close to each other, differences between corresponding values being roughly of the order of 1 per cent. One concludes at once that the change in characteristic impedance (Z_{02}') dominates by far over the series reactance X' in determining the values of r. It follows as a corollary that, since experimental values of X' are obtained by the use of the expression

$$X' = \left[\frac{Z_{02}'}{r}(r^2+1) - (Z_{02}'^2+1)\right]^{1/2}, \qquad (17)$$

X' is exceptionally sensitive to the smallest errors in both Z_{02}' and r. This was indeed found to be the case, in fact so much so that the experimental values of X' were completely unreliable. They have consequently not been included here. The theoretical values of X' are tabulated, however. While the experiments performed have not verified these theoretical values, they do indicate that the orders of magnitude of X' are correct.

The experimental values of l_1 and l_2 must be derived from measured data by formulas which, among other quantities, involve the (previously determined) experimental value of X'. In view of the unreliability of the experimental values of X', the derived values obtained for l_1 and l_2 were equally unreliable. Computations made using the theoretical X' in conjunction with other data obtained by measurement gave values for l_1 and l_2 ("semi-experimental") which appear quite reasonable. From these values (which are tabulated) one concludes that l_1 is indeed approximately equal to l_2 in magnitude and of opposite sign as the theoretical model predicts. It is seen, however, that the magnitudes involved are considerably smaller than $l_1 \simeq 0.23$ inch, as predicted for this case by (15). In all but one case ($w_1 = 1.204$, the most difficult to measure in this regard) l_1 and l_2 are, respectively, properly negative and positive. In view of these results, it is recommended that (15) be disregarded, and that for most purposes l_1 and l_2 be taken as zero.

The conclusions to be drawn from the preceding comparison of theory and experiment are: The step in strip line is very well approximated at T_0 by only the transformer ($\sqrt{Z_{02}'}$:1); the series reactance X' is negligible for almost all practical purposes, and the transmission lines ($l_1 = -l_2$) are small and unimportant.

G. Junction of Strip Transmission Line and Multistrip Transmission Line

The term multistrip transmission line has been employed previously[11] to refer to an infinite number of parallel, equispaced strips of identical widths symmetrically located between two ground planes. In the present context the term is used in the same fashion except that a *finite* number (m) of strips, with $m>1$, will be understood. The structure of interest is the junction between such a multistrip line and a (single center conductor) strip line as shown in Fig. 12.

A multistrip line can support $m+1$ different TEM modes, all of which, of course, have the same guide wavelength, *i.e.*, the free-space wavelength in the medium. In a two-strip line, for example, ($m=2$), three modes can propagate with electric fields as shown in Fig. 13.

The only mode under consideration here is the mode for which the fields surrounding each strip are almost identical to the field of the dominant (nonradiating) mode in (single center conductor) strip line. Such a mode is illustrated in Fig. 13(b) and Fig. 14 for $m=2$ and $m=4$, respectively. To distinguish this mode from all other modes in multistrip line, it will be arbitrarily referred to here as the "A mode." The junction in question then is that between usual strip line and the "A mode" in multistrip line.

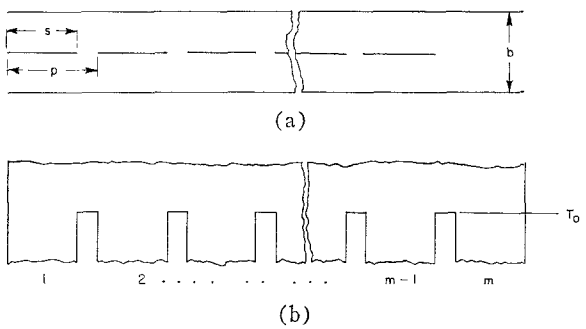

Fig. 12—Multistrip transmission line. (a) Cross section view. (b) Top view of center conductor.

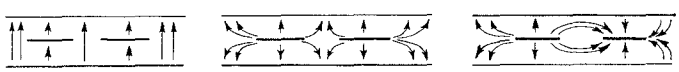

Fig. 13—Modes in a two-strip line. (a) Parallel plate (radiating) mode. (b) Even two-strip mode. (c) Odd two-strip mode.

Fig. 14—"A mode" in multistrip line with $m=4$.

It can be justifiably argued that the equivalent circuit representation of the strip-to-multistrip A-mode junction consists primarily of a (change of characteristic impedance) transformer. The representation should also include a series reactance, a small reference plane shift from the physical junction plane, and some small loss parameter(s) due to mode conversion. Experience

[11] A. A. Oliner and W. Rotman, "Periodic structures in trough waveguide," IRE TRANS. ON MICROWAVE THEORY AND TECHNIQUES, vol. MTT-7, pp. 134–140; January, 1959.

with the step in strip transmission line, however, strongly indicates that these additional parameters are quite small, so that the transformer alone at the plane T_o is an adequate representation for most purposes. This representation is shown in Fig. 15.

A previous result[11] for the case $m=\infty$ gives an expression for $Z_{o\infty}/Z_o$ based on a Babinet equivalence argument which uses the known susceptance of a capacitive slit in rectangular waveguide as a basis. This formula is

$$\frac{Z_{o\infty}}{Z_o} = 1 + \frac{2p}{\pi b} \ln \csc \frac{\pi s}{2p} . \tag{18}$$

By making use of this expression and the notion that the field in the multistrip line (m finite) is identical with the fields in the m infinite case everywhere except at the "outer" halves of strips 1 and m, one can derive a similar formula for m finite. The field associated with the two "outer" half-strips in this case can be regarded as the field of a (single) strip transmission line of width s. The resulting expression is

$$\frac{Z_{om}}{Z_o} = \frac{Z_{o\infty}/Z_o + A}{1 + A} , \tag{19}$$

where

$$A = \frac{K(k')}{K(k)} \frac{p}{mb} ; \quad k = \tanh\left(\frac{\pi s}{2b}\right), \quad k' = \sqrt{1 - k^2}.$$

The function K is the complete elliptic integral of the first kind. It can be seen that in the limiting cases of $m=0$ and $m=\infty$, the ratio Z_{om}/Z_o properly reduces to unity and to $Z_{o\infty}/Z_o$.

The measurement of Z_{om}/Z_o can be accomplished with relatively good accuracy; in addition, A is a constant which depends only on the known geometry of the multistrip line. In view of the simple formula relating these quantities to $Z_{o\infty}/Z_o$, the latter can be derived readily from the experimental value of Z_{om}/Z_o. The quantity $Z_{o\infty}/Z_o$ is of particular interest in context with certain periodic structures.[8]

Measurements on a six-strip transmission line were carried out to determine the parameters of the function at T_o with the objective of deriving $Z_{o\infty}/Z_o$ from the measured Z_{om}/Z_o value. Six was thought to be a sufficiently large number to satisfy reasonably well the inherent assumption that all but strips 1 and m are fed by a uniform field. The strip was measured at a wavelength $\lambda=7.830$ inches; the various dimensions were $b=1.051$ inches, $s=0.136$ inch, and $p=0.272$ inch. An average of three precision measurements gave the results which are compared in Table II with the corresponding theoretical values. The results of the experiment also indicated, as one would expect, that both reference planes of the transformer are in fact located slightly to the left of T_o (see Fig. 15); the left reference plane by approximately 0.05 inch, the right by about 0.04 inch.

The formula for Z_{om}/Z_o for $m=2$ involves the characteristic impedance of the even two-strip mode shown in Fig. 13(b), for which an exact result is available in the literature.[12] In terms of the notation employed in the reference cited, $Z_{02}/Z_o = Z_{oe}/2Z_o$. Because the multistrip formula for Z_{om}/Z_o can be expected to be least accurate in the two-strip case, it was compared to the exact two-strip formula. This comparison is presented graphically in Fig. 16. Since even in this worst case the correspondence is relatively good, it is felt that the multistrip formula can be usefully employed when $m=3$ or 4 and that it should be quite accurate for $m>4$.

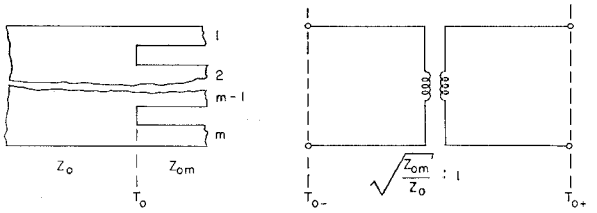

(a) (b)

Fig. 15—Junction between strip and multistrip transmission lines. (a) Top view of center conductor. (b) Simplified equivalent circuit.

TABLE II

	Z_{om}/Z_o	$Z_{o\infty}/Z_o$
Experimental	1.0535 ± 0.005	1.0588 ± 0.0055
Theoretical	1.0522	1.0573

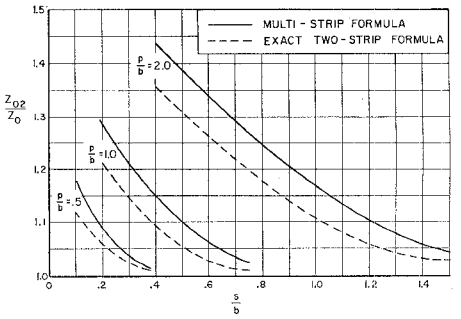

Fig. 16—Comparison between exact two-strip formula and multistrip formula for $m=2$ (worst case).

When a multistrip line is abruptly ended, an electrical open circuit will be located a small distance beyond the physical end as in the single center conductor case (see Fig. 4). Measurements were carried out on a multistrip line $m=6$, $b=1.051$ inches, $s=0.136$ inch, $p=0.272$ inch, at $\lambda=7.830$ inches to determine d, the distance from the end of the conductor to the electrical open circuit. The distance d was found to be 0.165 inch ± 0.015 inch. No theoretical expression for d is available. The number, however, falls roughly into the range one would expect by comparing it to the abruptly ended single strip case (see Fig. 5).

[12] S. B. Cohn, "Shielded coupled-strip transmission line," IRE TRANS. ON MICROWAVE THEORY AND TECHNIQUES, vol. MTT-3, pp. 29–38; October, 1955.

H. Sharp Bends: Arbitrary Angle, Right Angle

The parameters of sharp bends in the center conductor of strip line were measured as a function of angle θ for a single strip width and again as a function of strip width w for a single angle (90°). These two sets of measurements are presented essentially separately below.

The physical structure of the *arbitrary angle bend* and two alternative equivalent circuits are shown in Fig. 17.

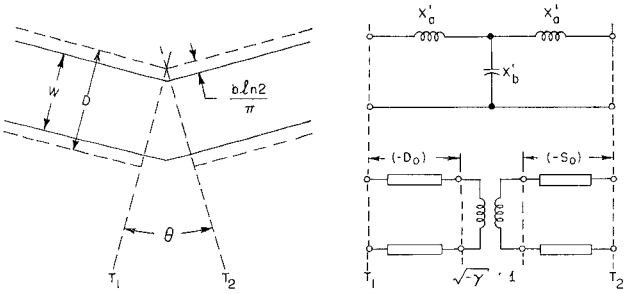

(a) (b)

Fig. 17—Sharp bend of arbitrary angle in center conductor. (a) Physical structure. (b) Two alternative equivalent circuits.

The reactance tee network involves the normalized reactances X_a' and X_b' which are obtained directly from theory. The theoretical parameters of the "tangent" (or transformer) network, however, are based on the values of X_a' and X_b'. The tangent network is a more useful representation for a bend since $-\gamma$ equals the insertion VSWR of the structure. It should be noted that reference planes T_1 and T_2, which are perpendicular to the strip on the two sides of the bend, intersect at the inside corner of the equivalent width strip (width D) rather than at the inside corner of the physical strip itself.

The theoretical formulas for X_a' and X_b' were derived[1] from the results for an E-plane bend in parallel plate waveguide by means of a Babinet equivalence procedure. These formulas are

$$X_b' = -\frac{\lambda}{2\pi D}\cot(\theta/2), \tag{20}$$

$$X_a' = \frac{2D}{\lambda}\left[\psi(x) + 1.9635 - \frac{1}{x}\right], \tag{21}$$

where, with θ in degrees,

$$x = \frac{1}{2}\left(1 + \frac{\theta}{180}\right), \qquad \frac{1}{2} < x < 1.$$

The function $\psi(x)$ is tabulated.[13]

[13] E. Jahnke and F. Emde, "Table of Functions," Dover Publications, Inc., New York, N. Y., p. 16; 1945.

The expressions required for abstracting the parameters of the tangent network (γ, D_o, and S_o) from those of the tee are

$$-\gamma = C + \sqrt{C^2 - 1}, \tag{22}$$

where

$$C = \frac{1 + 2(X_a' + X_b')^2 + X_a'^2(X_a' + 2X_b')^2}{2X_b'^2},$$

$$\kappa D_o = \tan^{-1}\alpha, \tag{23}$$

where

$$\alpha = \frac{\gamma - X_a'(X_a' + 2X_b')}{(X_a' + X_b')(1 + \gamma)},$$

$$\kappa S_o = \kappa D_o \pm \pi/2. \tag{24}$$

For θ small ($c \simeq 1$),

$$-\gamma \simeq 1 - \left(2X_a' + \frac{1}{X_b'}\right), \qquad \alpha \simeq \frac{1}{X_b'} - 1. \tag{25}$$

Theoretical and experimental results are compared in Figs. 18 and 19. The solid curves represent the theoretical results as computed from the formulas already given, *i.e.*, based upon the theoretical expressions for the parameters of E-plane bends in rectangular waveguide. The dashed curve (for $\theta > 60°$) for X_a' on the other hand is based upon *experimentally* obtained values for the parameters of E-plane bends in rectangular waveguide. Part of the discrepancy between (solid line) theory and experiment is consequently due to errors existing already in the theoretical result (X_a' only) for the rectangular waveguide bend. The discrepancy between (strip line) experiment and the dashed curve is somewhat larger. This is ascribed to an imperfection in the Babinet equivalent model for the bend in the following respect. In contrast to the Babinet model, which has impenetrable walls, the actual strip line possesses a fringing field which permits an additional small interaction to occur between the center conductor on one side of the bend and that on the other. This effect, which the Babinet model cannot account for, becomes more marked as the bend angle θ becomes larger.

For the small bend angles ($\theta < 30°$) the expressions for abstracting γ and D_o from X_a' and X_b' become quite sensitive and can lead to unreasonably large computational errors. The small angle approximations of these formulas, however, are very good, and in fact are substantially more reliable than the more "exact" expressions in this range. The theoretical values for γ and D_o obtained by their use are shown in the form of dot-dash curves. The $-\gamma$ vs θ curve is especially interesting in that it shows very graphically that it is advantageous to employ two or three smaller bends in place of one larger angle bend. For example, consider the experimental points at $\theta = 30°$, 45°, and 90°. The 90° bend has an insertion VSWR of 1.75; two 45° bends in tandem

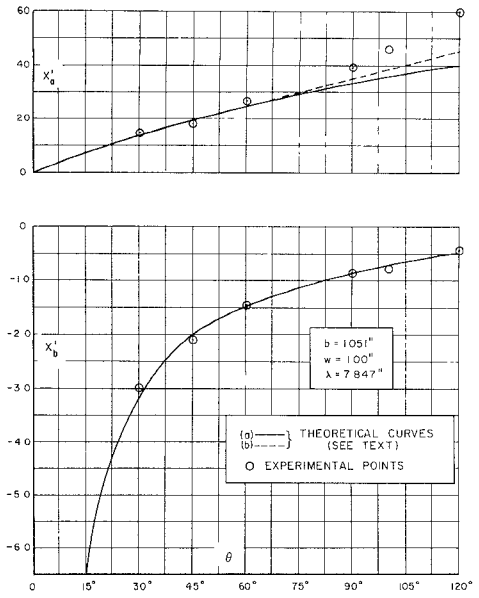

Fig. 18—Reactance tee network parameters for sharp angle bends.

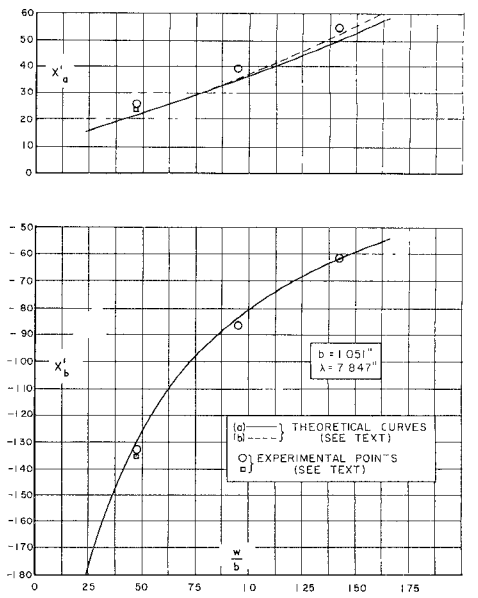

Fig. 20—Reactance tee network parameters for right-angle bends.

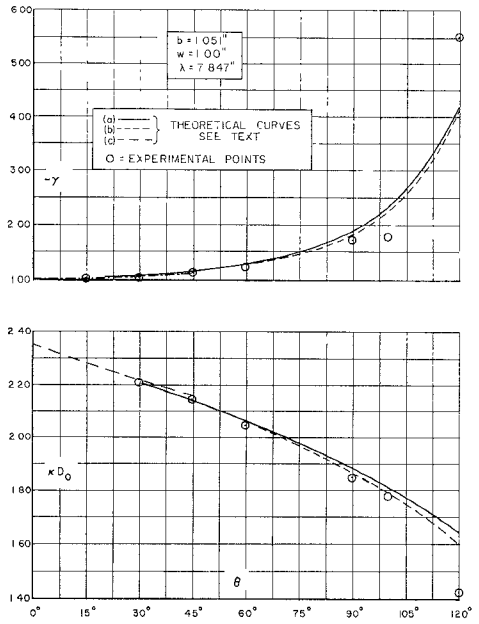

Fig. 19—Tangent network parameters for sharp angle bends

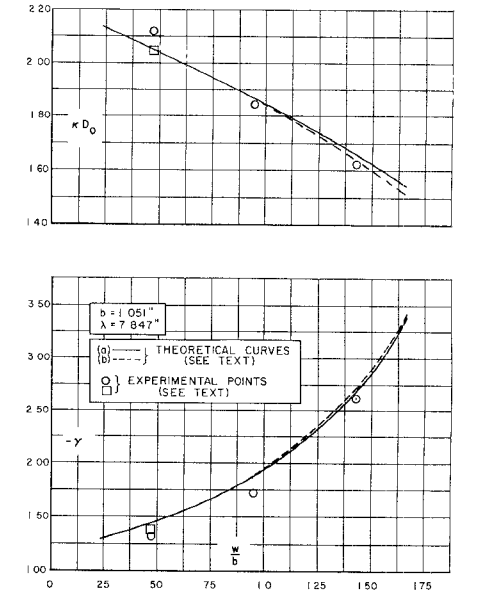

Fig. 21—Tangent network parameters for right-angle bends.

(and "far" from each other) can have a maximum insertion VSWR of 1.25; three 30° bends can have a maximum insertion VSWR of 1.15.

The *right-angle bend* is, of course, a special case of the arbitrary angle bend insofar as the physical structure and its equivalent circuit are concerned, *i.e.*, $\theta = 90°$ (see Fig. 17). The theoretical formulas have again been obtained[1] via a Babinet equivalence procedure, in this case from those for a right-angle E-plane bend in rectangular waveguide. The right-angle rectangular waveguide bend formula used as a basis is *not* a special case of the (rectangular waveguide) arbitrary angle bend formula, but is a more exact solution obtained especially for the 90° case. The right-angle bend formulas for X_a' and X_b' are given below. From these, the parameters γ, D_o, and S_o are, of course, abstracted as before by the use of (22) to (25).

$$X_a' = \frac{D}{\lambda}\left[1.756 + 4\left(\frac{D}{\lambda}\right)^2\right], \tag{26}$$

$$X_b' = 0.0725\left(\frac{D}{\lambda}\right) - 0.159/(D/\lambda). \tag{27}$$

Curves comparing theory and experiment are given in Figs. 20 and 21. As before, the solid line is based on

parameters for rectangular waveguide bends obtained by theoretical means and the dashed curves are the corresponding parameters obtained via rectangular waveguide measurements. As one would expect, the latter are in slightly better agreement with strip transmission line measurements than the strictly theoretical curves. In consequence of certain limitations of the measuring apparatus it was not possible to measure a single bend directly. Instead, either three or four (not necessarily similar) bends in tandem were measured at a time and the parameters for a single unknown bend were abstracted from the over-all data. The two experimental points shown for $w/b=0.475$ were obtained from two structures each consisting of four similar bends; however, the structures differed in that they involved different spacings between individual bends. The agreement between these two experimental points can be considered to be good in view of the many complications involved in the construction, measurement, and analysis of such four-bend structures.

I. Symmetric Tee Junction

The physical structure and the equivalent circuit for the symmetric tee junction are shown in Fig. 22. The symmetric arms of the tee structure are represented at the center line and the reactances X_a' and X_b' are normalized to Z_{01}. The representation of a symmetric lossless three-port in general requires four independent network parameters. In the representation employed here, one of these parameters is the length l of the transmission line which connects reference planes T_3 and T_3'. The approximate theory employed predicts, however, that l has a zero value. In consequence, the measured value of l directly expresses the error, if any, in the choice of T_3 as the plane at which the representation includes only the parameters X_a', X_b', and n.

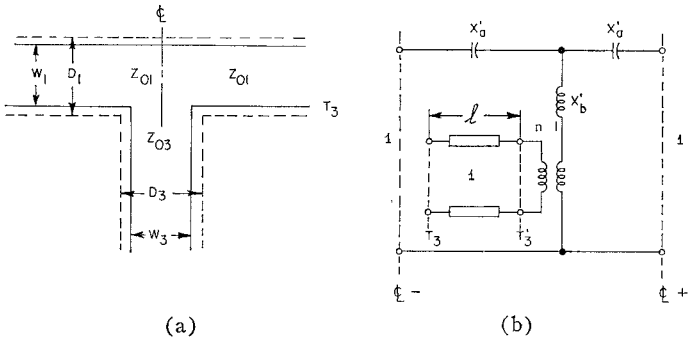

Fig. 22—Symmetric tee junction. (a) Physical structure. (b) Equivalent circuit.

The theoretical formulas (for X_a', X_b', and n) which have been available[1] were found to be adequate for X_a' and n. New expressions for X_b' have been derived, however, since the earlier formula had a very limited range of application. The present (as well as the earlier) formulas have been obtained via a Babinet equivalence procedure using known results for the parameters of the E-plane rectangular waveguide tee as a basis. They are

$$n' = \frac{\sin(\pi D_3/\lambda)}{(\pi D_3/\lambda)}; \qquad n = n'\sqrt{\frac{D_3}{D_1}}, \tag{28}$$

$$X_a' = -\frac{D_3}{\lambda}[0.785n]^2, \tag{29}$$

$$l = 0, \tag{30}$$

$$X_b' = -\frac{X_a'}{2} + \frac{1}{(n')^2}\left\{\frac{B_t}{2Y_o} + \left(\frac{2D_1}{\lambda}\right)\cdot\left[\ln 2 + \frac{\pi D_3}{6D_1} + \frac{3}{2}\left(\frac{D_1}{\lambda}\right)^2\right]\right\} \quad \text{for } \frac{D_3}{D_1} < 0.5, \tag{31}$$

where

$$\frac{B_t}{2Y_o} = \left(\frac{2D_1}{\lambda}\right)\left[\ln \csc\left(\frac{\pi D_3}{2D_1}\right) + \frac{1}{2}\left(\frac{D_1}{\lambda}\right)^2 \cos^4\left(\frac{\pi D_3}{2D_1}\right)\right],$$

$$X_b' = -\frac{X_a'}{2} + \frac{2D_1}{(n')^2\lambda}\left[\ln\left(\frac{1.43D_1}{D_3}\right) + 2\left(\frac{D_1}{\lambda}\right)^2\right] \quad \text{for } \frac{D_3}{D_1} > 0.5. \tag{32}$$

Seven tee structures with identical main line center strip widths, but with different stub line center strip widths, were measured. Measurements on strip line tee junctions have also been made at the Stanford Research Institute[14] with the objective of obtaining a compensated tee structure by empirical means. Their results have not been compared with the above formulas since a different equivalent circuit was employed by them.

Comparison of theory and measurement is shown in Figs. 23 and 24. The various parameters are plotted against the ratio of "main line" characteristic impedance to "stub line" characteristic impedance (Z_{01}/Z_{03}). This ratio equals D_3/D_1, where D_1 and D_3 are, respectively, the "equivalent widths" of the main line and stub line center conductors [see (1) to (4)]. As can be seen, the agreement for n is excellent. The series reactance X_a' is quite small and consequently relatively unimportant; the rather large percentage discrepancy between theory and experiment for X_a' can be expected in view of the difficulty of measuring such small parameters in a com-

[14] S. B. Cohn, *et al.*, "Design Criteria for Microwave Filters and Coupling Structures," Stanford Res. Inst., Menlo Park, Calif., Tech. Rept. No. 3; April 1–July 1, 1958.

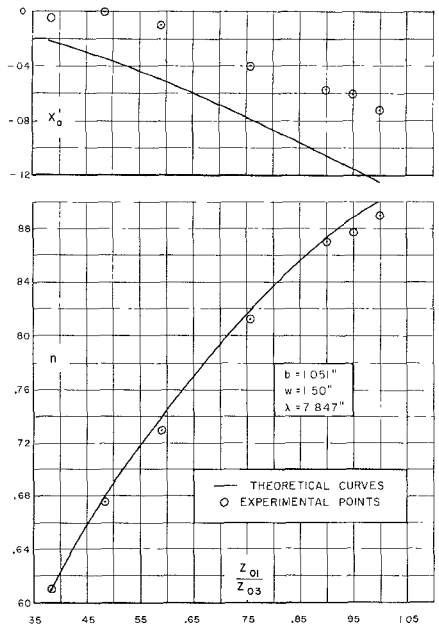

Fig. 23—Two of the circuit parameters for the symmetric tee junction.

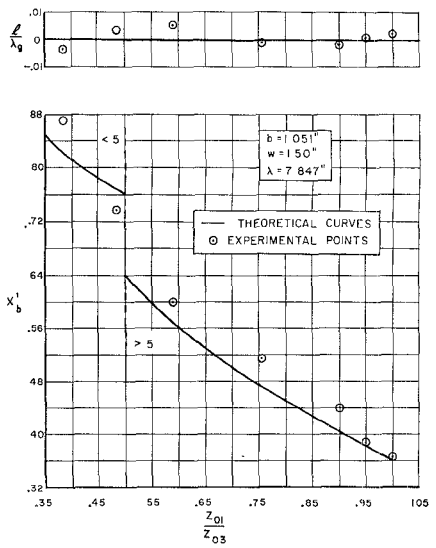

Fig. 24—The remaining two circuit parameters for the symmetric tee junction.

plicated structure in the presence of more significant parameters. The agreement for X_b' is actually much better (5 per cent or less) than a first glance at the curve would indicate. The two sections of the X_b' curve were computed by the formulas appropriate to the respective ranges. The experimentally determined length of line l (which is presented in Fig. 24 as normalized to guide wavelength) is seen to be sufficiently small to confirm the corresponding theory, *i.e.*, the terminals of the transformer are located so close to T_3 that line l is not required in the representation.

ACKNOWLEDGMENT

The authors wish to acknowledge the participation of M. Stillman, H. Hanft, S. Chertoff, and L. Horowitz in various phases of this work.

A Variational Integral for Propagation Constant of Lossy Transmission Lines*

ROBERT E. COLLIN†

Summary—**By assuming that the current on a lossy transmission line flows in the axial direction, only a variational integral for the propagation constant can be readily obtained. This variational integral shows that the usual power loss method of evaluating the attenuation constant is valid for general transmission lines. This variational integral also shows that the perturbation of the loss-free phase constant is due to the increase in magnetic field energy caused by penetration of the field into the conductors.**

* Manuscript received by the PGMTT, November 25, 1959; revised manuscript received, January 20, 1960. This work was supported in part by Air Force Cambridge Res. Center Contract AF19(604)3887.

† Elec. Engrg. Dept., Case Institute of Technology, Cleveland, Ohio.

INTRODUCTION

THE dominant mode of propagation on a loss-free transmission line is a TEM wave. In the transverse plane both the electric field and magnetic field may be derived from the gradients of suitable scalar functions of the transverse coordinates. The current flows entirely in the axial direction. Practical lines have finite conductivity and hence finite losses. As a consequence, there must be a component of the Poynting vector directed into the conductors and this in turn implies at least a longitudinal component of electric field. In general, longitudinal components of